Supplementary Information

N-doped hollow $Fe_{0.4}Co_{0.6}S_2$@NC nanoboxes derived from Prussian blue analogue as sodium ion anode

Ping Wan,[a] Shijie Wang, [a] Shuang Zhu, [a] Changda Wang, [a] Zhen Yu, [a] Wenjie Wang, [a] Yang Si, [a] Wangsheng Chu, * [a] and Li Song, [a]

[a] *National Synchrotron Radiation Lab, University of Science and Technology of China, Hefei, Anhui 230029, People's Republic of China*

*E-mail: chuws@ustc.edu.cn

Experimental

1. Synthesis of Precursor PBAs-Co nanocubes

In a typical procedure, 302.54 mg $Na_4[Fe(CN)_6]\cdot 10H_2O$ was dissolved into 125 mL deionized water. 1.875 g $C_6H_5Na_3O_7\cdot 2H_2O$ and 297.40 mg $CoCl_2\cdot 6H_2O$ were dissolved into 125 mL deionized water. Then mixed the two with stirring. The obtained solution was kept away from light for 24 h after stirred for 5-10 min. Later, green solids can be obtained by centrifuging and washing for several times with deionized water and ethanol. They were finally dried overnight at 120 °C under vacuum.

2. Synthesis of PBAs-Co@ PDA nanocubes

200 mg PBAs-Co nanocubes and 100 mg PDA were dissolved into 200 mL of Tris-buffer solution (10 mM) with magnetic stirring for 4 h. The resultant product was collected via centrifugation and washed with deionized water, and dried overnight at freeze dryer.

3. Synthesis of hollow FCSNC nanoboxes and FCS nanoparticles

The samples were prepared by high-temperature sintering in a tube furnace under Ar atmosphere. The as-prepared PBAs-Co@ PDA nanocubes and sulfur powder were loaded in the combustion boat with the sulfur totally submerging PBAs-Co@ PDA powders. A glass plate was partially covered on the combustion boat with the downstream side opening. Ar gas (500 sccm) was initially flowed into the tube for 1 h to remove the air. Then, the samples were annealed at 500 °C for 3 h with a heating rate of 2 °C·min^{-1} under Ar atmosphere with a flow rate of 200 sccm. After cooling to ambient temperature, the black solid products were rinsed with carbon disulfide and then harvested by centrifugation with DI water and ethanol for several times, and finally dried overnight at 120 °C under vacuum.

For the fabrication of compared samples, precursor PBAs-Co nanocubes without doping PDA were sulfuretted through the same sulfidation process.

4. Materials characterization

We used a D8-Advance power diffractometer equipped with a Cu Kα radiation source (λ = 1.54178 Å) to record XRD patterns of samples. The morphology of these samples was characterized by a field emission scanning electron microscopy (15 kV, JEOL, JSM-6700F) and TEM (JEOL JEM2010). The samples for SEM and HRTEM analysis were prepared by dispersion of the sample powders in ethanol. Few drops of the dispersed solution were spread onto a carbon film supported copper grid. Both of the SEM and HRTEM samples were prepared in air. Thermogravimetry (TG) measurement was carried out on a DTG-60H analyser in O2 flux at a scan rate of 10 °C

min^{-1}, from room temperature to 800 ℃. Element distribution was measured with an Optima 7300DV inductively coupled plasma – optical emission spectrometry (ICP-OES). X-ray photoelectron spectroscopy (XPS) measurement was performed in the Thermo ESCALAB 250 X-ray photoelectron spectrometer.

Fe K-edge X-ray absorption near edge structure (XANES) data was recorded at the 1W2B beamline of the Beijing Synchrotron Radiation Facility (BSRF, Beijing), and analysed by the ATHENA software package. To get the desired electrodes, the coin cells have been disassembled by an electric crimping machine (MTI Co.) after charged/discharged to the desired cut-off voltages. Finally, electrodes were washed with dimethyl carbonate (DMC) and sealed by a 3 M sellotape in Ar atmosphere after drying.

5. Electrochemical measurements

The battery tests were carried out in a half-cell configuration. The working electrode consists of active materials, conductivity agent (Ketjenblack), and polymer binder (polyvinylidene fluoride, PVDF) with a weight ratio of 7:2:1. After mixed fully in N-methyl-2-pyrrolidinone, the obtained slurry was casted on Cu foil and dried at 110°C under vacuum overnight. The typical loading mass of the active material was about 1.5 mg/cm^2. The electrolyte was a solution of 1 M $NaClO_4$ in polycarbonate with 5 % fluoroethylene carbonate (FEC) additive. Sodium disc was used as a counter electrode to assemble the CR2032-type coin cells, and all the processes were carried out in a glovebox filled with argon (MBraun, Germany). Whatman Glass Microfibre Filter (Grade GF/D) were used as separator. The electrochemical performance of the cells

was assessed on a Land CT2001A cell test system (Wuhan, China) in the range of 0.01-3.0 V (vs. Na^+/Na). Cyclic voltammetry was measured from 0.01 to 3.0 V (vs. Na^+/Na) at the scan rate of 0.1 mV s^{-1}. Electrochemical impedance spectroscopy (EIS) testing with an amplitude of 10 mV from 10^6 Hz to 0.01 Hz and Cyclic voltammetry (CV) curves of cells were obtained on a CHI660D (Chenhua, Shanghai) electrochemical workstation.

Rusults and discussion

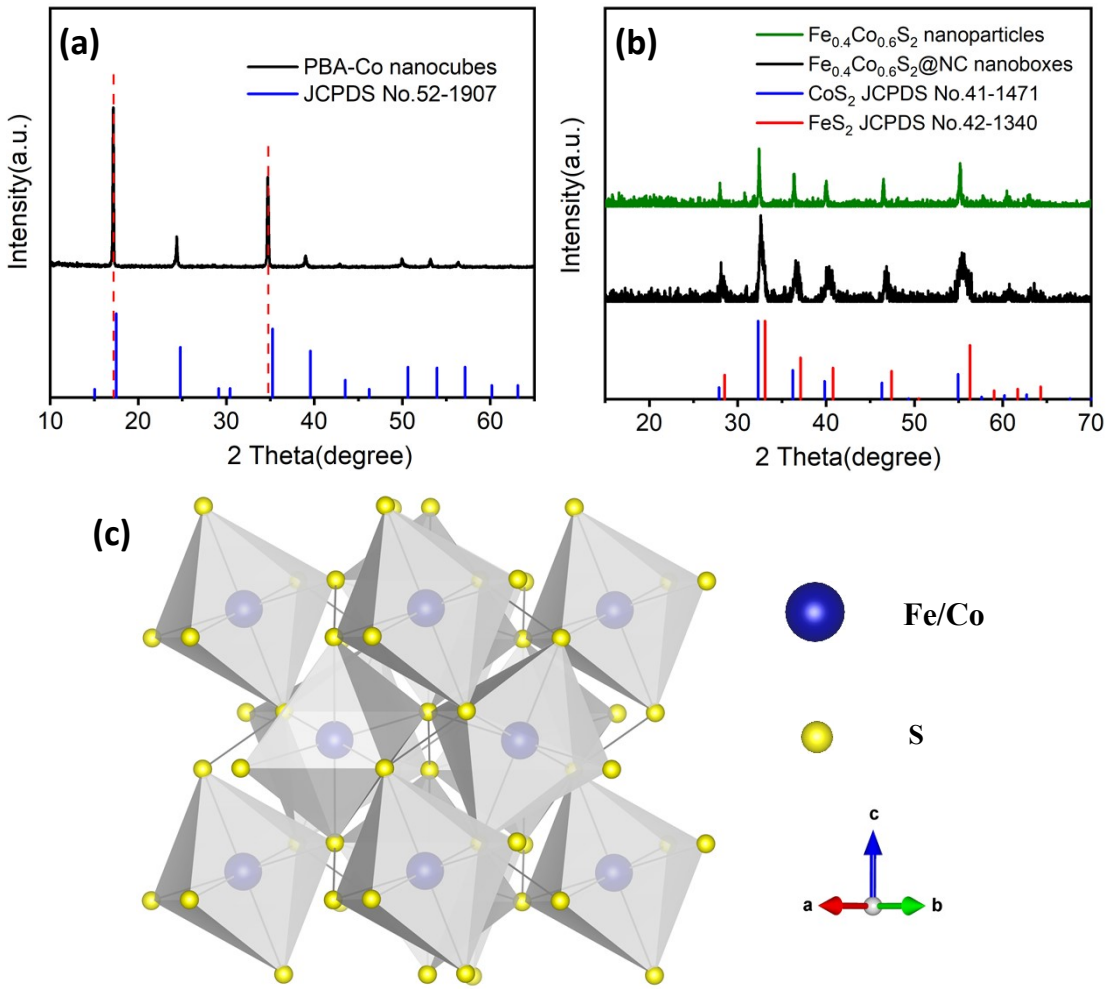

Fig. S1 XRD patterns of (a) precursor PBAs-Co nanocubes and (b) FCSNC nanoboxes

and FCS nanoparticles; (c) Lattice structure diagram of FCSNC nanoboxes and FCS nanoparticles.

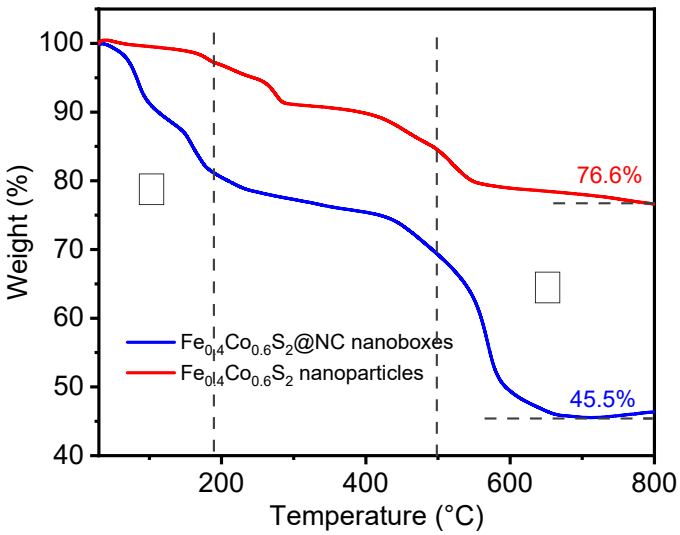

Fig. S2 Thermogravimetric curves of FCSNC nanoboxes and FCS nanoparticles.

After heating up to 800 ℃ under oxygen, the weight of the solid residues (Fe_3O_4 and Co_3O_4) of FCSNC and FCS accounted for 76.6% and 45.5%, respectively. The lower percentage of residues of FCSNC indicates the successful doping of nitrogen-doped carbon. When compared with FCS, FCSNC has two different obviously weight loss at about ① under 200 ℃ and ② 500-800 ℃.

It is worth noting that the weight of FCSNC dropped obviously under 200 ℃, in contrast to the basically unchanged weight of FCS. The possible reason is the weight loss might belong to elemental sulfur and water adsorbed in porous carbon. Owing to the high adsorption of porous carbon, in addition to physically adsorbed water, there might be slight sulfur vapor condensation on the sulfides surface during the cooling procedure, which is similar as the calcination of Se powder [1]. Although the sulfur is usually stable under 200 ℃, it could be combusted under 200 ℃ after distribution in the porous carbon because of the increased specific surface area. The elemental sulfur could be removed through more rinsing with carbon disulfide.

As for the second weight loss process at 500-800 ℃, the main reason is the combustion of the nitrogen-doped carbon, and the oxidation of FeS_2 to Fe_3O_4, CoS_2 to Co_3O_4.

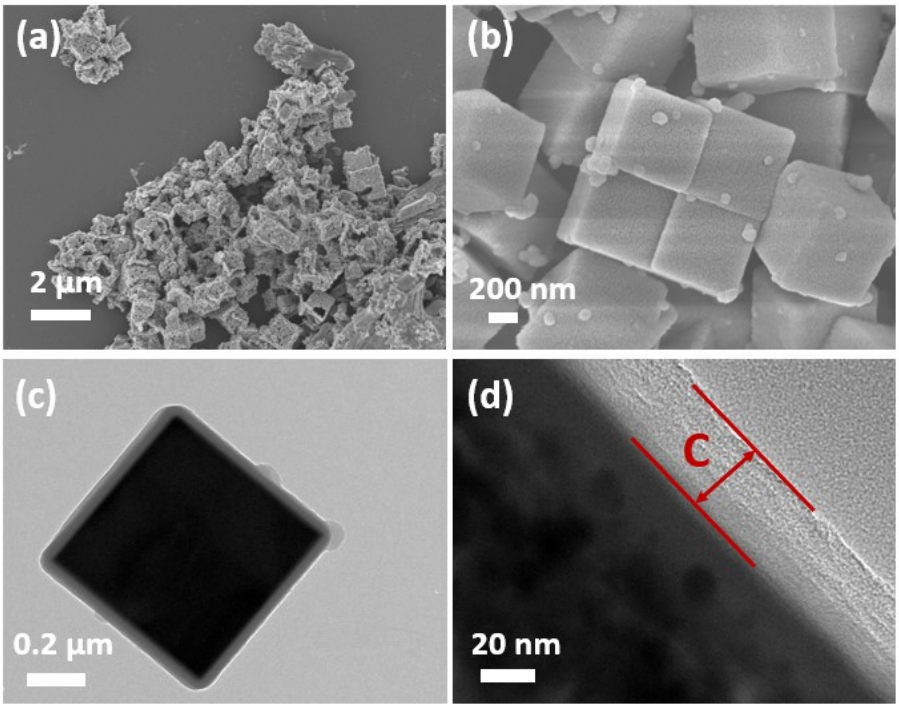

Fig. S3 (a) FESEM images of the FCS nanoparticles; (b) FESEM images and (c) TEM images of the PBAs-Co@PDA nanocubes; (d) The thickness of the PDA wrapped around the outer edge of PBAs-Co@PDA nanocubes.

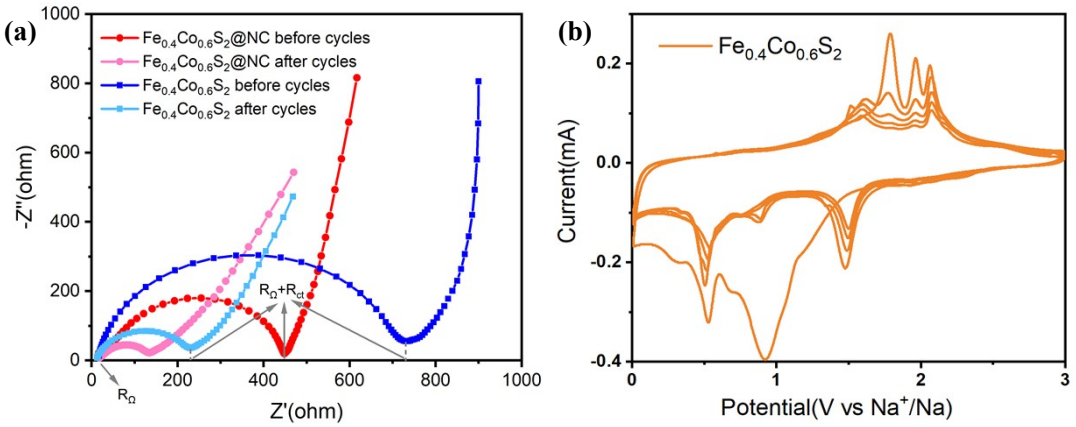

Fig. S4 (a) The impedance spectra of FCSNC nanoboxes and FCS nanoparticles before and after 100 cycles at 1 A/g; (b) Cyclic voltammetry data of the FCS nanoparticles anode.

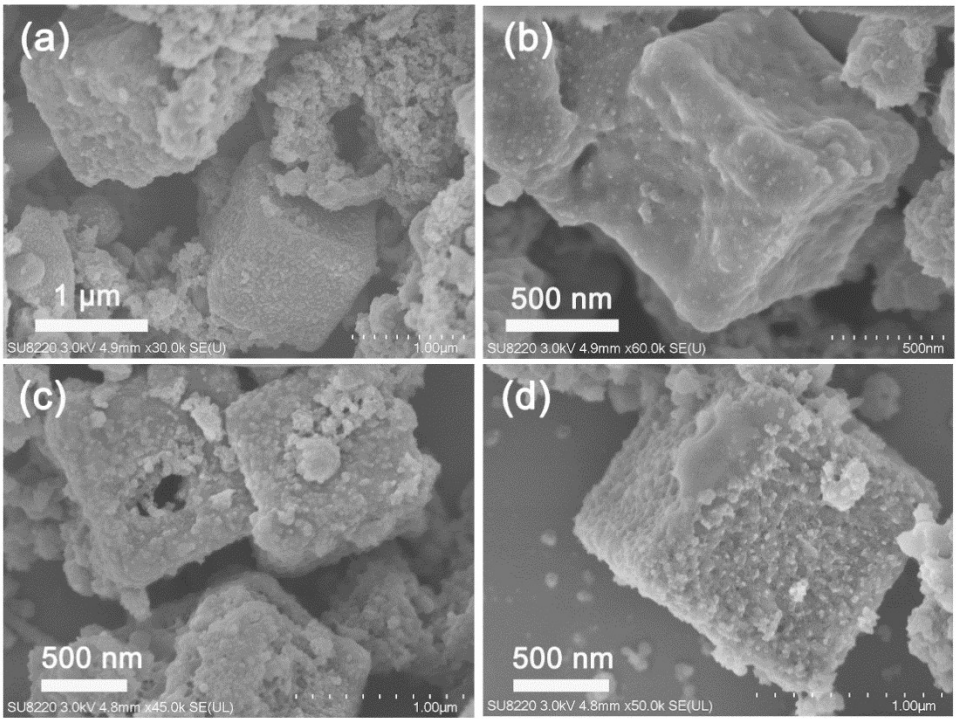

Fig. S5 FESEM images of the FCSNC nanoboxes anode after 300 cycles (a, b) and 500 cycles (c, d) at 1 A/g.

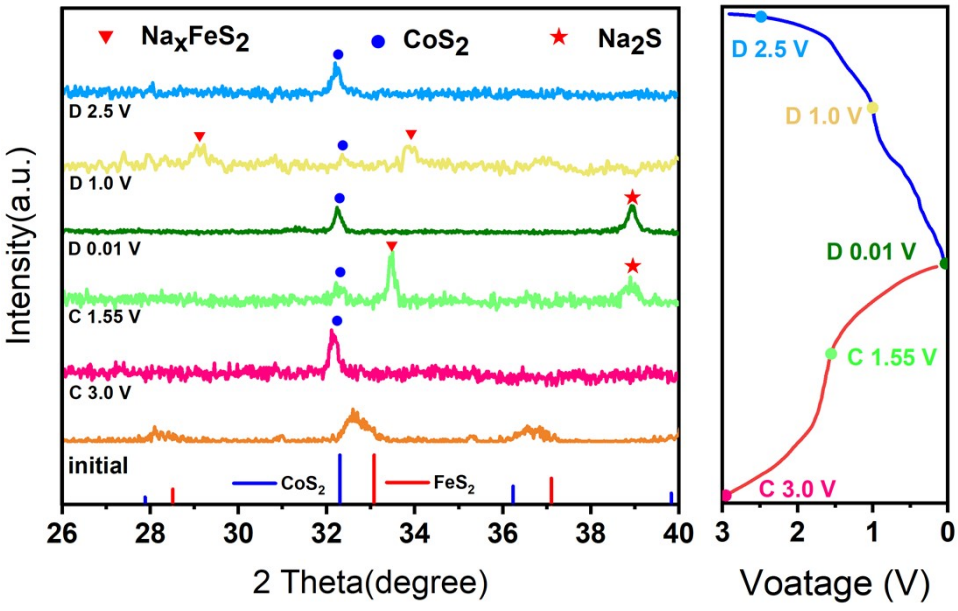

Fig. S6 Ex-situ XRD patterns at different voltage states during the second cycle of the FCSNC nanoboxes anode.

Except for the peak of CoS_2, no other peaks were observed when the anode was discharged to 0.01 V and charged to 3.0 V. It reveals that the complete conversion of the FeS_2 results in a final ultrasmall product [2].

Table S1 The ICP data of the FCSNC nanoboxes and FCS nanoparticles.

	Fe	Co	Fe/Co molar ratio
FCSNC (ppm)	**2.085**	**2.869**	**0.42/0.58**
FCS (ppm)	**3.107**	**4.027**	**0.44/0.56**

Table S2 The XPS data of the FCS nanoparticles.

	BE [eV]	Atomic conc. [%]
N 1s	**396.86**	**0.0**
Fe 2p	707.56	5.5
Co 2p	778.86	6.6
S 2p	162.86	34.7
C 1s	284.76	53.2

Table S3 Performances of recently reported SIBs based on iron or cobalt sulfides.

Materials	**Electrolytes** [a)]	**Voltage, V (*vs.* Na^+/Na)**	**Capacity, mAh/g**	**Cycling stability** [b)]	**Refs.**
FeCo8S8 NS/rGO	1 M $NaCF_3SO_3$ /DEGDME	0.4-2.9	188 @ 20 A/g	220@100@10 A/g	3
FeCoS2	1 M $NaPF_6$/EC-DMC	0-3.0	806 @ 50 mA/g	420@20@50 mA/g	4
$FeCoS_4$@CNTGH	1 M $NaPF_6$/ DME	0.005-2.5	745 @ 500 mA/g	680@1000@2 A/g	2
Mesoporous FeS2@C particles	1 M $NaCF_3SO_3$/DGM	0.8-3.0	244 @ 10 A/g	329@1000@0.2 A/g	5
yolk-shell FeS2@carbon microboxes	1 M $NaCF_3SO_3$/DGM	0.5-3	237@5 A/g 200@10 A/g	257@1000@0.5 A/g	6
FeS2@CNT	1 M $NaClO_4$/PC-EC +5%FEC	0.01-2.0	277@5 A/g	410@250@1 A/g	7
Marcasite FeS_2 hollow	1 M $NaCF_3SO_3$/DGM	0.8-2.8	242@5 A/g 174@10 A/g	363@300@0.1 A/g	8

microspheres					
CoS2-C/CNT	1 M $NaPF_6$/DME	0.01-3.0	306 @ 2 A/g	403@200@0.1 A/g	9
CNT @ CoS @ C	1 M $NaClO_4$/EC-DEC +5%FEC	0.005-3.0	278 @ 5 A/g	415@100@0.1 A/g	10
Co_9S_8/Co	1 M $NaCF_3SO_3$/TEGDGM+5% FEC	0.2-2.5	173.4 @ 10 A/g	78.4% capacity retention @1000@10 A/g	11
$Fe_{0.4}Co_{0.6}S_2$@NC	**1 M $NaClO_4$/EC-DEC +5%FEC**	**0.01-3.0**	**295.8 @ 5 A/g 252.7@10 A/g**	**230@900@10 A/g**	**This work**

[a] (EC: ethylene carbonate; DEC: diethyl carbonate; FEC: fluoroethylene carbonate; PC: propylene carbonate; TEGDME: tetraethylene glycol dimethyl ether); [b] (Cycling stability is expressed as the percentage of energy storage capacity retention after several charging/discharging cycles at a specific rate).

Supplementary Reference

1. D. W. Sha, C. J. Lu, W. He, J. X. Ding, H. Zhang, Z. H. Bao, X. Cao, J. C. Fan, Y. Dou , L. Pan and Z. M. Sun, ACS Nano, 2022, 16, 2711-2720.
2. Z. Hao, N. Dimov, J.-K. Chang and S. Okada, Chem. Eng. J., 2021, 423, 130070.
3. S. Lu, J. Jiang, H. Yang, Y. J. Zhang, D. N. Pei, J. J. Chen and Y. Yu, ACS Nano, 2020, 14, 10438-10451.
4. Y. Zhao, J. Liu, C. Ding, C. Wang, X. Zhai, J. Li and H. Jin, CrystEngComm, 2018, 20, 2175-2182.
5. L. Yao, B. Wang, Y. Yang, X. Chen, J. Hu, D. Yang and A. Dong, Chem. Commun., 2019, 55, 1229-1232.
6. P. Jing, Q. Wang, Q. Y. Wang, X. Gao, Y. Zhang and H. Wu, Carbon, 2020, 159, 366-377.
7. Y. Liu, L. Zhang, D. Liu, W. Hu, X. Yan, C. Yu, H. Zeng and T. Shen, Nanoscale, 2019, 11, 15497–15507.
8. X. L. Wu, H. Q. Zhao, J. M. Xu, W. Wang, S. G. Dai, T. T. Xu, S. M. Liu, S. Zhang, X. C. Wang and X. J. Li, Journal of Alloys and Compounds, 2020, 528, 154173.
9. Y. Ma, Y. Ma, D. Bresser, Y. Ji, D. Geiger, U. Kaiser, C. Streb, A. Varzi and S. Passerini, Acs Nano, 2018, 12, 7220-7231.
10. F. Han, C. Zhang, B. Sun, W. Tang, J. Yang and X. Li, Carbon, 2017, 118, 731-742.
11. Y. Zhao, Q. Pang, Y. Wei, L. Wei, Y. Ju, B. Zou, Y. Gao and G. Chen, Chemsuschem, 2017, 10, 4778-4785.